Optical absorption edge and luminescence in phosphorous-implanted Cu$_6$PS$_5$X (X = I, Br) single crystals

I.P. Studenyak[1], V.Yu. Izai[1], V.O. Stephanovich[1], V.V. Panko[1], P. Kúš[2], A. Plecenik[2],
M. Zahoran[2], J. Greguš[2], T. Roch[2]
[1]*Uzhhorod National University, Physics Faculty,*
46, Pidhirna str. 88000 Uzhhorod, Ukraine
[2]*Comenius University, Faculty of Mathematics, Physics and Informatics,*
Mlynska dolina, 84248 Bratislava, Slovakia
E-mail:studenyak@dr.com

Abstract. Implantation of Cu$_6$PS$_5$X (X = I, Br) single crystals was carried out for different values of fluence with using P$^+$ ions; the energy of ions was 150 keV. For the implanted Cu$_6$PS$_5$X crystals, the structural studies were performed using the scanning electron microscopy technique and energy-dispersive X-ray spectroscopy. Spectrometric studies of optical absorption edge and luminescence were carried out within the temperature range 77…320 K. The influence of ionic implantation on luminescence spectra, parameters of Urbach absorption edge, parameters of exciton-phonon interaction as well as ordering-disordering processes in Cu$_6$PS$_5$X (X = I, Br) superionic conductors have been studied.

Keywords: superionic crystal, implantation, absorption edge, Urbach rule, exciton-phonon interaction, luminescence.

1. Introduction

Cu$_6$PS$_5$X compounds with argyrodite structure are characterized by high ionic conductivity and well known as ferroelastic and nonlinear optical materials [1]. They are promising materials for creation of solid electrolyte power sources, electrochemical and optical sensors [2]. At room temperature, they belong to the cubic syngony $F\bar{4}3m$ [1, 3]. The specific features of Cu$_6$PS$_5$X crystal structure and phase transitions are studied in [1−4].

It should be noted that the electrical, acoustic, calorimetric and some optical properties of Cu$_6$PS$_5$X compound have been studied quite extensively [2, 5-7]. Near the optical absorption edge in Cu$_6$PS$_5$X crystals, the excitonic bands are revealed, which are smeared with temperature increase and Urbach behaviour of absorption edge is observed [2]. In the luminescence spectra of Cu$_6$PS$_5$X crystals at low temperatures, the excitonic and impurity-related bands are observed; with temperature increase the noticeable temperature quenching takes place [8].

This paper is aimed at the optical absorption and luminescence studies of implanted Cu$_6$PS$_5$X superionic crystals as well as the influence of implantation on Urbach parameters, parameters of exciton-phonon interaction and ordering-disordering processes.

2. Experimental

Cu$_6$PS$_5$X single crystals were grown using chemical vapour transport [2]. Implantation of Cu$_6$PS$_5$X crystals with P$^+$ ions was performed using an experimental set-up with magnetic separation and variable accelerating voltage [9]: the energy of ions was 150 keV, the angle of incidence was 10°.

For the implanted Cu$_6$PS$_5$X crystals, the structural studies were performed using scanning electron microscopy technique (Hitachi S-4300) and energy-dispersive X-ray spectroscopy. It was shown that on the surface of implanted Cu$_6$PS$_5$X crystals the darkened areas with linear size of 100 up to 200 nm are created, and their amount increases with fluence. Phosphorous

implantation does not lead to the remarkable changes in chemical composition of Cu_6PS_5X crystals.

Spectrometric studies of optical absorption edge and luminescence were carried out within the temperature range 77 to 320 K using LOMO KSVU-23 grating monochromator; for the luminescence studies the 532-nm laser light was used as the excitation source [2, 8]. During the measurements, the samples were oriented at room temperature while being in the cubic phase. For low temperature studies cryostat of UTREX type was used, stability and accuracy of temperature measurements were ±0.5 K. The relative error in determination of the absorption coefficient $\Delta\alpha/\alpha$ did not exceed 10% at $0.3 \le \alpha d \le 3$ [2].

3. Results and discussion

Fig. 1 presents spectral dependences of the absorption coefficient for unimplanted and implanted Cu_6PS_5X crystals at 300 K for various fluences. It is shown that the optical absorption edge for both unimplanted and implanted Cu_6PS_5X crystals has an exponential shape. The inset (Fig. 1) shows the dependences of such parameters of the absorption edge as optical pseudogap E_g^* (E_g^* is the absorption edge energy position at the fixed value of the absorption coefficient $\alpha = 10^3 \, \text{cm}^{-1}$) and the Urbach energy E_U (E_U is the energy width of the exponential absorption edge) on the fluence. It has been revealed for Cu_6PS_5X crystals that E_g^* very slightly changes with the fluence increase (for Cu_6PS_5I crystals the tendency of the slight nonlinearly decreasing is observed, as well as for Cu_6PS_5I crystal, contrary, the tendency of the slight nonlinearly increasing is observed). With fluence increase, the Urbach energy E_U in Cu_6PS_5X crystal slightly increases as compared to the unimplanted crystals (by 4-5%), and then decreases (by 6%) for Cu_6PS_5I crystals and increases (by 17%) for Cu_6PS_5Br crystals. The latter is the evidence for structural ordering in Cu_6PS_5I crystals, which increases at ion implantation, while in Cu_6PS_5Br crystals the structural disordering of crystal lattice with implantation is observed.

The temperature studies of optical absorption edge have shown that the temperature behaviour of exponential parts at the absorption edge in unimplanted and implanted Cu_6PS_5X crystals for $T > T_I$ follows the Urbach rule [10]:

$$\alpha(h\nu, T) = \alpha_0 \cdot \exp\left[\frac{\sigma(h\nu - E_0)}{kT}\right] = \alpha_0 \cdot \exp\left[\frac{h\nu - E_0}{E_U(T)}\right], \quad (1)$$

where σ is the steepness parameter, α_0 and E_0 are the convergence point coordinates of the Urbach bundle, $h\nu$ is the photon energy. Fig. 2 presents spectral dependences of the absorption coefficient at various

temperatures for the implanted Cu_6PS_5I (by the fluence 1×10^{15} ions/cm^2) and Cu_6PS_5Br (by the fluence 1×10^{13} ions/cm^2) crystals. It should be noted that the similar Urbach bundles are observed for all the implanted Cu_6PS_5X crystals. The coordinates of the Urbach bundle convergence point α_0 and E_0 for the implanted crystals at various fluence values are given in Tables 1 and 2. For comparison, Tables 1 and 2 contain corresponding parameters for the unimplanted Cu_6PS_5X crystal.

The exponential shape of the absorption edge longwave side is usually related to exciton-phonon interaction (EPI) [11]. Within the whole investigated temperature interval, for all the implanted Cu_6PS_5X crystals (Fig. 2), the temperature dependences of the absorption edge steepness parameter $\sigma = kT/E_U$, where k is the Boltzmann constant, T is temperature, are described by the Mahr relation [11]:

$$\sigma(T) = \sigma_0 \cdot \left(\frac{2kT}{\hbar\omega_p}\right) \cdot \text{th}\left(\frac{\hbar\omega_p}{2kT}\right), \quad (2)$$
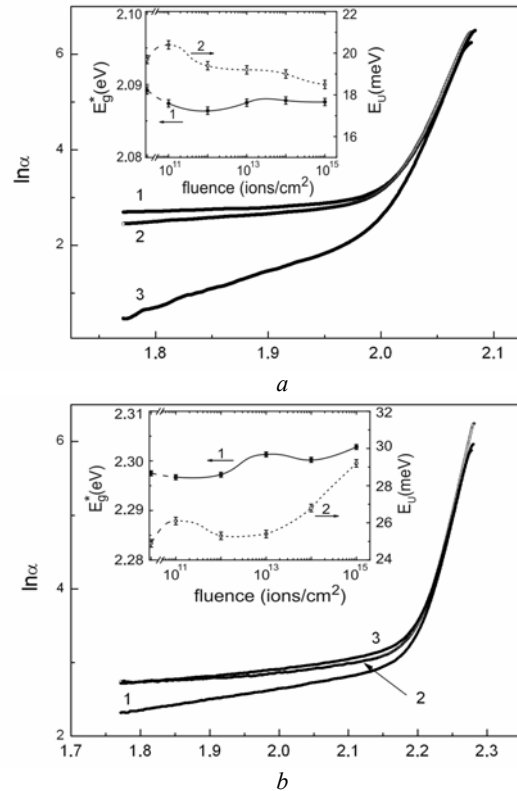

a

b

Fig. 1. Spectral dependences of the absorption coefficient for unimplanted and implanted Cu_6PS_5I (a) and Cu_6PS_5Br (b) crystals at $T = 300$ K and various fluences: (1) unimplanted crystal, (2) 1×10^{12} and (3) 1×10^{14} ions/cm^2. The inset shows dependences of the optical pseudogap E_g^* (1) and Urbach energy E_U (2) on fluence for implanted Cu_6PS_5I and Cu_6PS_5Br crystals.

where the σ_0 parameter is a constant independent of temperature and related to the EPI constant g as $\sigma_0 = 2/3g$; $\hbar\omega_p$ is the effective average phonon energy in a single-oscillator model, describing the EPI [11]. The values of the effective phonon energy $\hbar\omega_p$ taking part in formation of the absorption edge, and the σ_0 parameter are given in Tables 1 and 2. It should be noted that for the implanted Cu_6PS_5X crystals, like for the unimplanted one, the value σ_0 is higher than unity (except for Cu_6PS_5Br crystal at the fluence 1×10^{15} ions/cm^2), which indicates weak EPI [12]. The dependences of the EPI parameter σ_0 and the effective average phonon energy $\hbar\omega_p$ on fluence for the implanted Cu_6PS_5X crystals are presented in Fig. 3,

besides their behaviour is opposite for Cu_6PS_5I and Cu_6PS_5Br crystals. Thus, for Cu_6PS_5I crystals with increase of fluence the σ_0 parameter increases by 10% and at fluences higher than 1×10^{12} ions/cm^2 obtains the constant value, while the effective phonon energy $\hbar\omega_p$ at this fluence has its maximum. In the implanted Cu_6PS_5Br crystals, the σ_0 parameter with fluence nonlinearly decreases by 11%, while the effective phonon energy $\hbar\omega_p$ at fluence of 1×10^{13} ions/cm^2 has its minimum.

The temperature dependences of the optical pseudogap E_g^* and the Urbach energy E_U for Cu_6PS_5I crystal implanted at the fluence of 1×10^{15} ions/cm^2 as well as for Cu_6PS_5Br crystal implanted at the fluence of

Table 1. Parameters of the Urbach absorption edge and parameters of exciton-phonon interaction for unimplanted and phosphorous-implanted Cu₆PS₅I crystals.

Crystal Cu_6PS_5I	Unimplanted	1×10^{11} ions/cm^2	1×10^{12} ions/cm^2	1×10^{13} ions/cm^2	1×10^{14} ions/cm^2	1×10^{15} ions/cm^2
E_g^* (300K) (eV)	2.0892	2.0874	2.0864	2.0875	2.0878	2.0876
E_U (300K) (meV)	19.7	20.4	19.4	19.2	19.0	18.5
α_0 (cm^{-1})	4.7×10^5	4.3×10^5	6.9×10^5	6.3×10^5	5.8×10^5	5.7×10^5
E_0 (eV)	2.211	2.211	2.213	2.211	2.209	2.204
σ_0	1.36	1.32	1.45	1.45	1.45	1.45
$\hbar\omega_p$ (meV)	17.1	18.6	25.0	21.5	18.9	18.5
θ_E (K)	198	216	290	250	251	215
$(E_U)_0$ (meV)	6.4	7.0	8.6	8.4	7.6	6.3
$(E_U)_1$ (meV)	12.8	14.1	17.2	16.8	14.7	12.7
E_g^* (0) (eV)	2.179	2.172	2.168	2.170	2.172	2.175
S_g^*	2.5	4.8	5.4	5.2	5.1	4.9

Table 2. Parameters of the Urbach absorption edge and parameters of exciton-phonon interaction for unimplanted and phosphorous-implanted Cu₆PS₅Br crystals.

Crystal Cu_6PS_5Br	Unimplanted	1×10^{11} ions/cm^2	1×10^{12} ions/cm^2	1×10^{13} ions/cm^2	1×10^{14} ions/cm^2	1×10^{15} ions/cm^2
E_g^* (300K) (eV)	2.2975	2.2967	2.2972	2.3013	2.3002	2.3028
E_U (300K) (meV)	24.9	26.1	25.3	25.4	26.8	29.2
α_0 (cm^{-1})	3.6×10^5	3.5×10^5	3.5×10^5	3.7×10^5	3.7×10^5	3.8×10^5
E_0 (eV)	2.446	2.450	2.447	2.451	2.461	2.478
σ_0	1.12	1.10	1.09	1.08	1.06	1.00
$\hbar\omega_p$ (meV)	26.1	30.4	23.9	22.5	28.1	32.1
θ_E (K)	303	353	277	261	326	372
$(E_U)_0$ (meV)	11.7	14.1	10.7	10.2	13.1	16.2
$(E_U)_1$ (meV)	23.1	26.9	22.2	21.1	27.0	31.8
E_g^* (0) (eV)	2.391	2.395	2.420	2.400	2.391	2.394
S_g^*	6.23	7.26	7.92	6.07	6.32	6.97
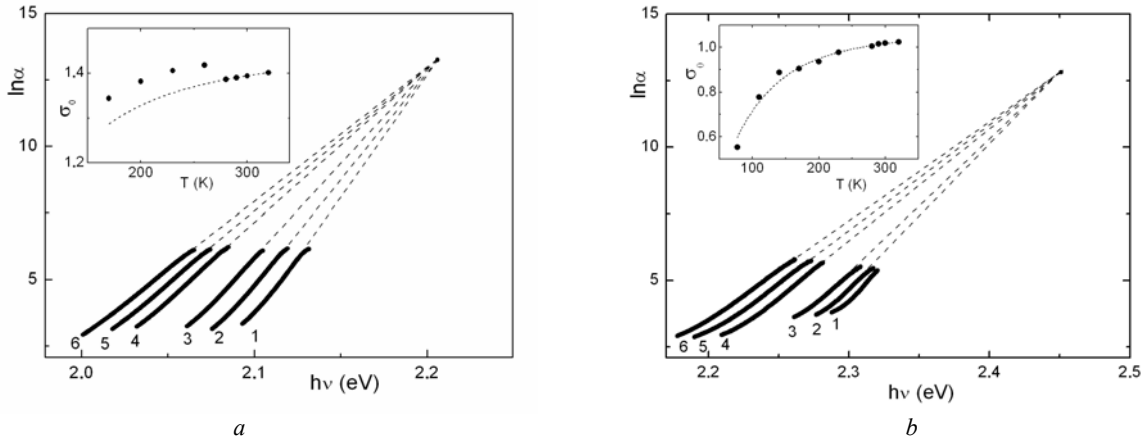
Fig. 2. Spectral dependences of the absorption coefficient for Cu_6PS_5I (a) and Cu_6PS_5Br (b) crystals, implanted by the fluence 1×10^{15} (a) and 1×10^{13} ions/cm² (b), at various temperatures: (1) 170, (2) 200, (3) 230, (4) 280, (5) 300, and (6) 320 K. The inset shows the temperature dependence of the steepness parameter σ.
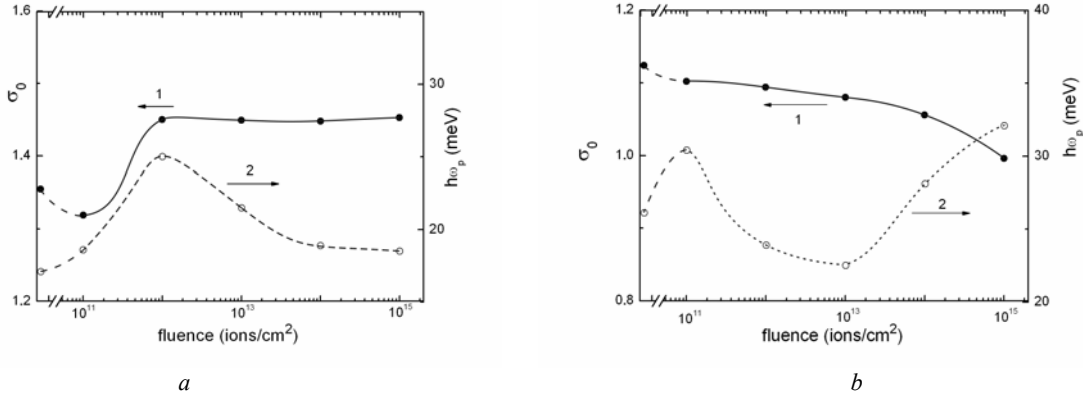

Fig. 3. Dependences of the σ_0 parameter (1) and energy of effective phonons $\hbar\omega_p$ (2) on the fluence for the implanted Cu_6PS_5I (a) and Cu_6PS_5Br (b) crystals.

1×10^{13} ions/cm² are presented in Fig. 4. It should be noted that the temperature behaviour of E_g^* and E_U for all the implanted Cu_6PS_5X (X = I, Br) crystals are well described in the Einstein model by equations [13, 14]:

$$E_g^*(T) = E_g^*(0) - S_g^* k\theta_E \left[\frac{1}{\exp(\theta_E/T)-1} \right], \qquad (3)$$

$$(E_U) = (E_U)_0 + (E_U)_1 \left[\frac{1}{\exp(\theta_E/T)-1} \right], \qquad (4)$$

where $E_g^*(0)$ and S_g^* are the energy gap at 0 K and a dimensionless constant, respectively; θ_E is the Einstein temperature, corresponding to the average frequency of phonon excitations of a system of non-coupled oscillators; $(E_U)_0$ and $(E_U)_1$ are constants. The performed calculations show that within the whole temperature range the experimental values of E_g^* and E_U are well described by Eqs. (3) and (4). The obtained $E_g^*(0)$, S_g^*, θ_E, $(E_U)_0$ and $(E_U)_1$ parameters for the unimplanted and implanted (with various fluences) crystals are given in Tables 1 and 2. The temperature dependences of the optical pseudogap E_g^* and Urbach energy E_U for Cu_6PS_5I crystal implanted with the fluence of 1×10^{15} ions/cm² as well as for Cu_6PS_5Br crystal implanted with the fluence of 1×10^{13} ions/cm², calculated from Eqs. (3) and (4), are shown in Fig. 4 as solid and dashed lines.

It should be noted that the Urbach absorption edge shape is determined by the temperature-related and structural disordering of crystal lattice, and Urbach energy E_U is described by the equation [15]

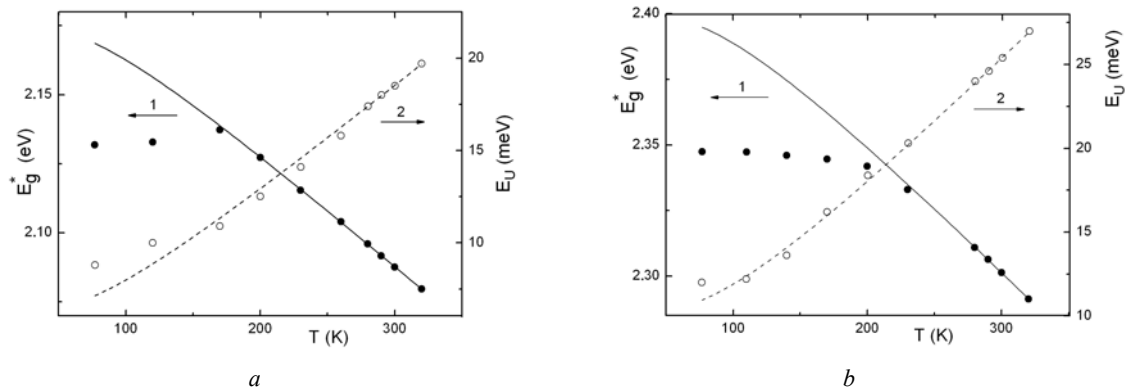$$E_U = (E_U)_T + (E_U)_X = (E_U)_T + (E_U)_{X,stat} + (E_U)_{X,dyn}, \qquad (5)$$

Fig. 4. Temperature dependences of the optical pseudogap E_g^* (1) and Urbach energy E_U (2) for Cu_6PS_5I (a) and Cu_6PS_5Br (b) crystals implanted with the fluence 1×10^{15} ions/cm^2.
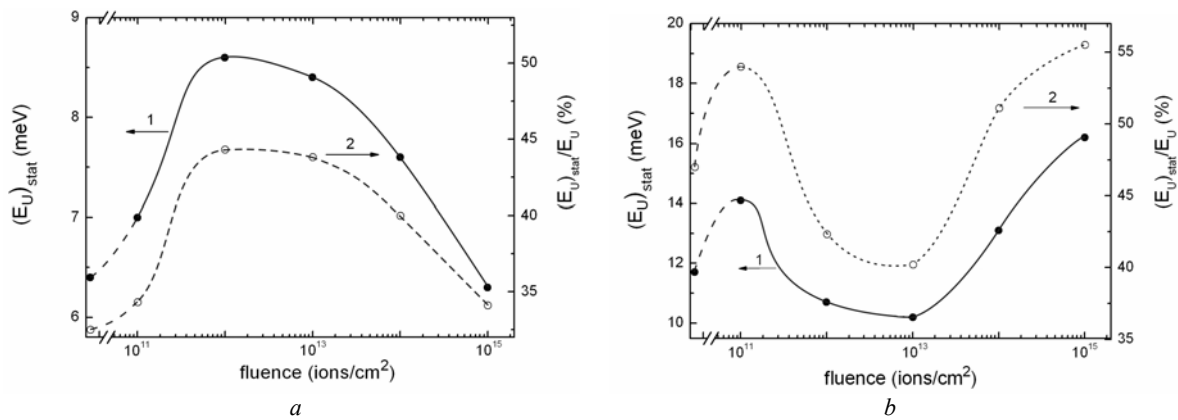

Fig. 5. Dependences of the absolute (1) and relative (2) values of contribution of static structural disordering into the Urbach energy E_U on the fluence for implanted Cu_6PS_5I (a) and Cu_6PS_5Br (b) crystals.
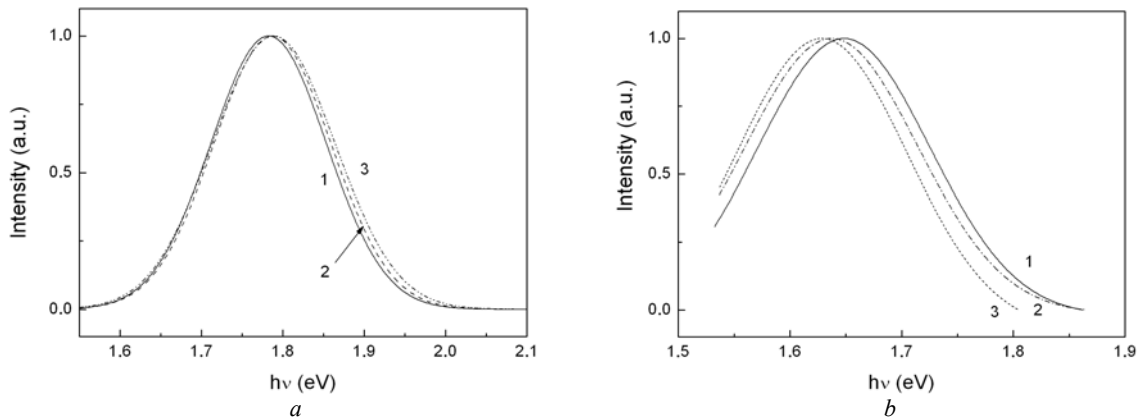
Fig. 6. Luminescence spectra of unimplanted and implanted Cu_6PS_5I (a) and Cu_6PS_5Br (b) crystals at $T = 77$ K and various fluences: (1) unimplanted crystal, (2) 1×10^{12}, (3) 1×10^{14} ions/cm^2.

where $(E_U)_T$ and $(E_U)_X$ are contributions of temperature-related and structural disordering to E_U, respectively; $(E_U)_{X,stat}$ and $(E_U)_{X,dyn}$ are contributions of static structural disordering and dynamic structural disordering to $(E_U)_X$, respectively. The static structural disordering $(E_U)_{X,stat}$ in Cu_6PS_5X crystal is caused by structural imperfectness due to the high concentration of disordered copper vacancies as well as the dynamic structural disordering $(E_U)_{X,dyn}$ is related to the intense motion of mobile copper ions, participating in ion transport, and is responsible for the ionic conductivity [2]. It should be noted that the first term in the right-hand side of Eq. (4) represents static structural

disordering, and the second one – temperature-related types of disordering: temperature disordering due to thermal lattice vibrations and dynamic structural disordering due to the presence of mobile ions in superionic conductors.

The contributions of temperature-related disordering and static structural disordering into the Urbach energy E_U for the implanted Cu_6PS_5X crystals were evaluated using the method that was developed in Ref. [2]. Thus, for Cu_6PS_5I crystal the dependence of absolute value of contribution of $(E_U)_{X,stat}$ on the fluence reveals its maximum at the fluence of 1×10^{12} ions/cm^2 (Fig. 5a). Similarly, with increase of fluence the relative contribution of static structural disordering into the Urbach energy increases from 32.5% (for unimplanted crystal), achives the maximum value of 44.3% (at the fluence 1×10^{12} ions/cm^2), and then decreases down to the value 34.1% (at the fluence 1×10^{14} ions/cm^2) (Fig. 5a). The reverse situation is observed for Cu_6PS_5Br crystal. It is shown that dependences of the absolute value for $(E_U)_{X,stat}$ contribution as well as its relative value on the fluence reveal their minimum at the fluence of 1×10^{13} ions/cm^2 (Fig. 5b). At the fluence 1×10^{15} ions/cm^2, the relative value of contribution of static structural disordering into the Urbach energy is 55.5%, while for the unimplanted crystal is 47% (Fig. 5b).

In the luminescence spectrum of unimplanted Cu_6PS_5I crystal, measured at the excitation by a semiconductor laser with $\lambda = 532$ nm at $T = 77$ K at the energy 1.783 eV, a wide impurity-related band is observed, which corresponds to a "band-to-local centre" transition (Fig. 6a). With increasing the temperature, there is a noticeable temperature luminescence quenching, the impurity luminescence band broadens, decreases in its intensity and completely smears out at 120 K. In the implanted crystals, the high-energy shift of impurity band and its broadening are observed (Fig. 6a). In the luminescence spectrum of the unimplanted Cu_6PS_5Br crystal at $T = 77$ K, a wide impurity-related band is revealed at 1.648 eV (Fig. 6b). Implantation of Cu_6PS_5Br crystals with phosphorous ions results in the band shift to the low energies and its broadening.

4. Conclusions

Cu_6PS_5X single crystals grown by chemical vapour transport were implanted using various fluences of 150-keV P$^+$ ions. It has been shown that the optical absorption edge of both unimplanted and implanted Cu_6PS_5X crystals is of exponential shape. In superionic phase, the Urbach behaviour of the optical absorption edge caused by exciton-phonon interaction is revealed. It has been shown that exciton-phonon interaction in both unimplanted and implanted Cu_6PS_5X crystals is weak, however, in implanted Cu_6PS_5I crystals it is diminished,

while in implanted Cu_6PS_5Br crystals it is strengthened. Temperature dependences of the optical pseudogap and Urbach energy, being well described in the framework of the Einstein model, are obtained. The contributions of static structural disordering, induced by ion implantation, into the Urbach energy have been evaluated. The influence of temperature and ion implantation on luminescence spectra has been studied as well as the mechanisms of radiative recombination in implanted crystals have been discussed.

References

1. W.F. Kuhs, R. Nitsche, and K. Scheunemann, Vapour growth and lattice data of new compounds with icosahedral structure of the type Cu_6PS_5Hal (Hal = Cl, Br, I) // *Mat. Res. Bull.* **11**, p. 1115-1124 (1976).
2. I.P. Studenyak, M. Kranjčec, and M.V. Kurik, Urbach rule and disordering processes in $Cu_6P(S_{1-x}Se_x)_5Br_{1-y}I_y$ superionic conductors // *J. Phys. Chem. Solids*, **67**, p. 807-817 (2006).
3. A. Haznar, A. Pietraszko, and I.P. Studenyak, X-ray study of the superionic phase transition in Cu_6PS_5Br // *Solid State Ionics*, **119**, p. 31-36 (1999).
4. A. Gagor, A. Pietraszko, and D. Kaynts, Diffusion paths formation for Cu^+ ions in superionic Cu_6PS_5I single crystals studied in terms of structural phase transition // *J. Solid State Chem.* **178**, p. 3366-3375 (2005).
5. R.B. Beeken, J.J. Garbe, and N.R. Petersen, Cation mobility in the Cu_6PS_5X (X = Cl, Br, I) argyrodites // *J. Phys. Chem. Solids*, **64**, p. 1261-1264 (2003).
6. S. Fiechter and E. Gmelin, Thermochemical data of argyrodite-type ionic conductors: Cu_6PS_5Hal (Hal = Cl, Br, I) // *Thermochimica Acta*, **85**, p. 155-158 (1985).
7. V. Samulionis, J. Banys, Y. Vysochanskii, and I. Studenyak, Investigation of ultrasonic and acoustoelectric properties of ferroelectric-semiconductor crystals // *Ferroelectrics*, **336**, p. 29-38 (2006).
8. I.P. Studenyak, R.Yu. Buchuk, V.O. Stephanovich, S. Kökényesi, and M. Kis-Varga, Luminescent properties of Cu_6PS_5I nanosized superionic conductors // *Radiation Measurements*, **42**, p. 788-791 (2007).
9. I.P. Studenyak, V.Yu. Izai, V.O. Stefanovich, V.V. Panko, P. Kúš, and A. Plecenik, On the Urbach rule in sulphur-implanted Cu_6PS_5I

superionic conductors // *J. Phys. Chem. Solids*, **71**, p. 988-992 (2010).

10. F. Urbach, The long-wavelength edge of photographic sensitivity and electronic absorption of solids // *Phys. Rev.* **92**, p. 1324-1326 (1953).

11. M.V. Kurik, Urbach rule (Review) // *Phys. Status Solidi* (*a*), **8**, p. 9-30 (1971).

12. H. Sumi and A. Sumi, The Urbach-Martiensen rule revisited // *J. Phys. Soc. Japan*, **56**, p. 2211-2220 (1987).

13. M. Beaudoin, A.J.G. DeVries, S.R. Johnson, H. Laman, and T. Tiedje, Optical absorption edge of semi-insulating GaAs and InP at high temperatures // *Appl. Phys. Lett.* **70**, p. 3540-3542 (1997).

14. Z. Yang, K.P. Homewood, M.S. Finney, M.A. Harry, and K.J. Reeson, Optical absorption study of ion beam synthesized polycrystalline semiconducting $FeSi_2$ // *J. Appl. Phys.* **78**, p. 1958-1963 (1995).

15. G.D. Cody, T. Tiedje, B. Abeles, B. Brooks, and Y. Goldstein, Disorder and the optical-absorption edge of hydrogenated amorphous silicon // *Phys. Rev. Lett.* **47**, p. 1480-1483 (1981).